

# Anti-arrhythmic Effects of Atrial Specific $I_{Kur}$ Block: A Simulation Study

P Law, S Kharche, J Higham, H Zhang

School of Physics and Astronomy, University of Manchester, Manchester, UK

## Abstract

The ultra rapid potassium current ( $I_{Kur}$ ) is an attractive pharmacological target in atrial fibrillation (AF) management due to its atrial specific nature. An experimentally based 78%  $I_{Kur}$  reduction was incorporated into a human atrial action potential (AP) model under sinus rhythm (SR) and atrial fibrillation (AF) conditions. Its effects on cell and tissue level electrical activity were simulated.

$I_{Kur}$  block reduced AP duration (APD) and effective refractory period (ERP) under SR conditions, but prolonged APD and ERP under AF conditions.  $I_{Kur}$  block modulated tissue's ability to sustain high pacing rate conduction under SR and AF conditions. Vulnerability window (VW) was augmented under SR, and reduced under AF conditions.  $I_{Kur}$  block did not effect on re-entrant waves in 2D and 3D simulations. Simulations show pro-arrhythmic effects in SR, but anti-arrhythmic effects in AF case due to  $I_{Kur}$  block.

## 1. Introduction

Atrial fibrillation (AF) is the most common arrhythmia and affects a large part of the elderly population in developed nations. Clinical management of atrial fibrillation (AF) is largely rhythm control and achieved by administration of Class I and III pharmacological agents [1, 2]. While interventions with such agents are common, their medium to long term effectiveness in maintaining sinus-rhythm (SR) is limited with suboptimal efficacy and adverse side effects [3]. Pharmacological agents aim to alleviate AF by blocking key atrial ion currents responsible for the atrial myocyte repolarisation thereby lengthening the action potential duration (APD) and effective refractory periods (ERP). Increased ERP lengthens the wavelength at which the tissue can sustain a re-entrant circuit and therefore limits the tissues susceptibility to the genesis of AF. However, the ventricles share many of the same ion channels as the atria therefore it is not possible to alter ion channel properties in the atria with out also altering the electrophysical properties of ventricular cells. This leads to adverse side effects of ventricular pro-arrhythmia.

Current drug development is increasingly focused on developing atrial specific pharmacological agents [4].

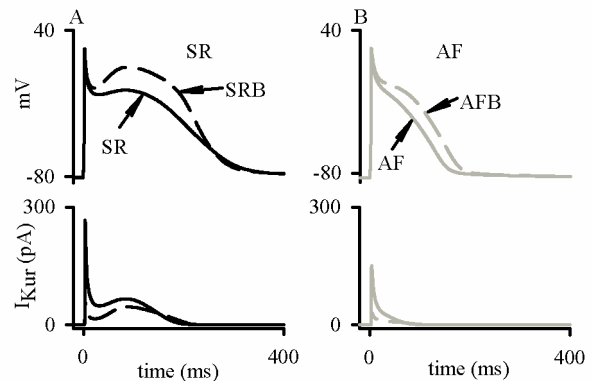


Figure 1 A: Top panel shows AP profiles under SR (solid line) and  $I_{Kur}$  blocked under SR (dashed line) conditions. Bottom panel shows the corresponding  $I_{Kur}$  during the AP. B: Top panel shows AP profiles under AF (gray line) and bottom panel shows the corresponding  $I_{Kur}$  traces during the AP.

The benefits of blocking  $I_{Kur}$  are being increasingly identified with pharmacological agents being developed to provide a robust AF therapy with minimal risk [5, 6]. It has been experimentally shown by Wettwer et al. [7] that low concentrations ( $\sim 10 - 50 \mu\text{M/L}$ ) of 4-aminopyridine (4-AP) selectively blocked  $I_{Kur}$  in human atrial myocytes without affecting properties of other ionic currents. They reported that an  $I_{Kur}$  block resulted in a shortening of APD. In contrast the application of 4-AP to AF cells was observed to give a modest increase in APD [7].

While previous experimental data [7] and simulation [8] studies have identified that blocking of  $I_{Kur}$  results in a shortening of APD, the full effects have not been studied in detail. The present multi-physics simulation study focused on quantifying the anti-arrhythmogenic effects of blocking  $I_{Kur}$  at cellular, tissue and organ levels under SR and AF conditions. This case study uses previously developed simulation environments [9].

## 2. Methods

The biophysically detailed model for human atrial

action potential (AP) developed by Courtemanche et al. [8] (CRN model) was implemented in the simulations. The model is well established and has been used in previous simulation studies [10-13]. The model was modified to simulate APs under normal SR conditions (standard CRN model),  $I_{Kur}$  block under SR conditions (SRB), AF due to ion channel remodelling, and  $I_{Kur}$  block under AF conditions (AFB). The  $I_{Kur}$  block was implemented as a 78% reduction of the  $I_{Kur}$  current based on experimental data [7]. AF was simulated as described in our previous studies [12, 14]. In brief, simulating AF consists of a 98% increase in the inward rectifying potassium current ( $I_{K1}$ ), a 61% reduction in the transient outward current ( $I_{to}$ ), a 68% reduction in the in the L-type calcium current ( $I_{CaL}$ ), a 52% reduction in the  $I_{Kur}$  current, and a 67% increase in the sodium-calcium exchanger pump ( $I_{NaCa}$ ).  $I_{Kur}$  block was simulated as a further 78% blocking of  $I_{Kur}$  under the SR or AF conditions. APs were evoked by a series of 10 conditioning supra-threshold stimuli at pacing cycle length (PCL) of 1 s, with strength 2 nA/pF and duration 2 ms. Such a conditioning was deemed sufficient to elicit further stable APs. The 11<sup>th</sup> AP was then noted for further analysis. APD was defined as the time interval taken from the 11<sup>th</sup> stimulus to the time when the evoked AP reached 90% repolarization. APD restitution (APDr) were computed using standard S1-S2 protocol where a premature stimulus (S2) was applied at a given time after the 10<sup>th</sup> conditioning stimulus of S1 (PCL = 1 s), as in our previous study [12]. Diastolic interval (DI) was defined as the time interval between 90% repolarization of the previous AP and the upstroke of the final AP. A plot of the measured APD against DI gave the APDr curves. Maximal slopes of the curves were determined. ERP was defined as the minimum S1-S1 stimulus interval that produced an AP with peak potential over 80% of that of the final S1 evoked AP [15]. ERP was simulated over a range of PCLs and ERP restitution (ERPr) curves were constructed.

The cell models were then incorporated into a reaction-diffusion parabolic partial differential equation (PDE) to construct 1D, 2D and 3D mono-domain models of spatially extended homogeneous atrial tissue. The parabolic PDE has the form

$$C_m \partial u / \partial t = D \nabla^2 u - I_{ion} \quad (1)$$

where  $C_m$  is cell membrane capacitance,  $D$  is the uniform electrotonic diffusive coupling that models the intercellular gap junctional electrical coupling,  $u$  is the membrane potential, and  $I_{ion}$  is the total membrane current. In the models,  $D$  was set to 0.031 mm<sup>2</sup>/ms to produce a physiological conduction velocity (CV) of 0.27 mm/ms in a solitary excitation wave under SR conditions [11]. In the 1D and 2D tissue models, the inter-cellular distance was taken to be 0.1 mm. Such a space step is close to the length of human atrial cells and is also sufficiently small to give stable numerical

solutions. The 1D strand model of homogenous atrial fibres had a length 20 mm, discretized to consist of 200 coupled cells. Using the 1D model, CV restitution (CVr) and temporal vulnerable window (VW) of the atrial tissue were computed using methods described in a previous study [11]. Re-entrant wave dynamics were studied using 2D and 3D models. Using stimulation protocols as in previous study [9], re-entrant excitation scroll waves were initiated. The anatomically detailed 3D model of human atria was developed in our previous study [13]. The 3D model has a spatial resolution of 0.33 mm x 0.33 mm x 0.33 mm. The models were numerically solved using the forward marching explicit Euler single step method with a constant time step of 0.005 ms, which gives accurate solutions without compromising computation time [9].

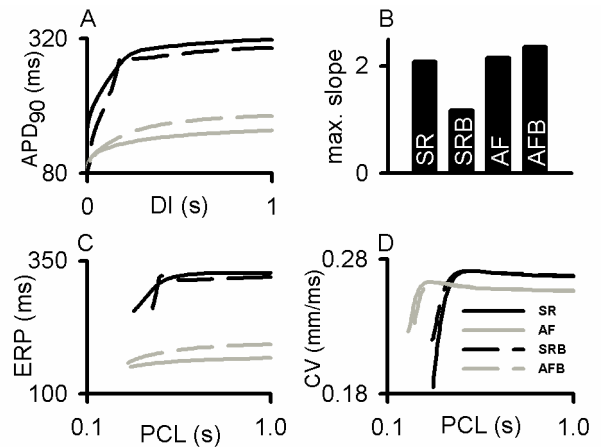


Figure 2 Effects of  $I_{Kur}$  block on cell and 1D model properties. A: APDr curves; B: Maximum slopes of APDr curves; C: ERPr curves; D: CVr curves.

### 3. Results

Solitary APs show an abbreviation due to  $I_{Kur}$  block under SR conditions, and a prolongation under AF conditions as shown in Figure 1. The SR APD of 314.13 ms was abbreviated to 299.2 ms under SRB conditions, and the characteristically short AF APD of 155.5 ms was prolonged to 180.6 ms under AFB conditions. APDr curves (Figure 2, A) show an increased maximal slope as shown in Figure 2, B. The maximal slopes under SR conditions were observed to be 2, to be 1.2 under SRB conditions, 2.15 under AF and 2.36 under AFB conditions. The rate dependence of the ERP is shown in Figure 2, C. Under SR conditions the ERP at a PCL of 1 s was measured to be 327.9 ms. Under SRB conditions the ERP was reduced by 2.5% to 319.8 ms indicating that  $I_{Kur}$  blocking increases the tissue's susceptibility to AF. However, a sudden dramatic reduction in ERP was observed at high PCLs and the cut off PCL is measured to be 417.7 ms, 27.1% higher than under SR conditions.

This indicates that blocking  $I_{Kur}$  under SR conditions provides an arrhythmogenic effect by reducing the ERP. Under AF conditions the ERP is reduced to be 167.7 ms which is 48.8% shorter than the SR case and the cut off BCL was measured to be 312.0 ms, a 5.1% reduction from the SR case. In the AFB case the ERP was found to be reduced by 41% at 193.5 ms and the cut off BCL was found to be reduced by 19.4% to 265.0 ms. The CVr curves are shown in Figure 2, D. Solitary wave CV under SR and SRB were measured to be 0.26 mm/ms, and CV in under AF and AFB was measured to be 0.25 mm/ms indicating that the  $I_{Kur}$  block did little to alter the CV at low pacing rates. However, CVr shows that SRB shifted the restitution curve in the negative direction, indicating an increased propensity to sustained wave propagation at high pacing rates, whereas AFB results in a shift of the CVr curve to the positive direction from the AF case indicating a loss of excitation propagation at high pacing lengths. This suggests that under AF conditions, blocking  $I_{Kur}$  has an anti-arrhythmogenic effect.

2D re-entry simulations are shown in Figure 3. Under SR conditions the lifespan (LS) of spiral waves was measured to be 1.4 s [9]. The dominant frequency (DF) of localized excitations was measured at 3 Hz and the tip meander area was 5.25 cm<sup>2</sup>. In contrast under AF conditions, the stable spiral wave persisted for the total simulated duration of 10 s. DF was increased to 8.2 Hz and the tip meander area was reduced to 4 cm<sup>2</sup>. Under SRB conditions, LS of the spiral wave was around 1 s. The measured DF was 4.6 Hz. However, the tip meander area was reduced substantially due to  $I_{Kur}$  block. Under AFB conditions the stability and persistence of the spiral wave was unaffected as compared to the AF case.

3D simulations along with time traces and dominant frequency are shown in Figure 4. Under SR conditions, scroll waves self-terminated after 4.2 s and the DF was measured to be 3 Hz. Under SRB conditions, a moderate reduction of LS and DF from SR conditions to 4.1 s and 2.6 Hz respectively. In the AF case scroll waves persisted for the simulated period of 10 s, and had a DF of 7.4 Hz. In case of AFB, the re-entrant wave persisted for the period of the simulation and the DF was also reduced from AF conditions to 6 Hz. The anti-arrhythmic properties of the  $I_{Kur}$  blocking were observed in a reduction of the power of the re-entrant wave.

#### 4. Conclusions and discussion

This simulation study shows that  $I_{Kur}$  channel blocking under normal SR conditions results in a reduction of APD and ERP which increases arrhythmogenicity. However, blocking of  $I_{Kur}$  under AF conditions prolongs AP and increases ERP. While simulations in the single cell indicate the anti-arrhythmic effects of blocking the  $I_{Kur}$  current, re-entrant dynamics in the 2D and 3D simulations

show that blocking  $I_{Kur}$  does not play a significant role in the dissipation of re-entrant spiral waves. However, in the 2D simulation the tip-meander area is reduced substantially. This suggests that the blocking of the  $I_{Kur}$  channel alone is not effective in alleviating the onset of AF and surgical intervention is required.

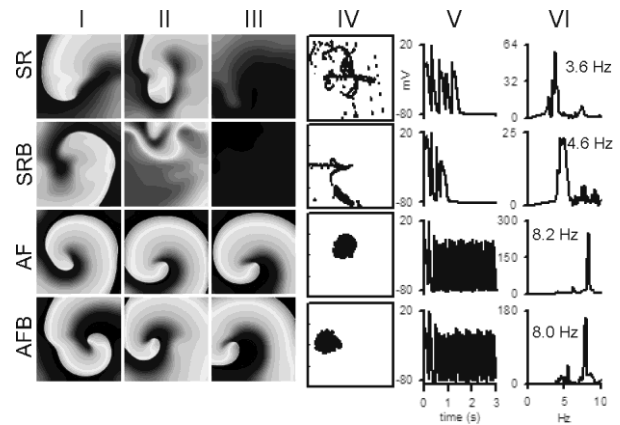


Figure 3 Re-entry in 2D homogenous sheets of human atrial tissue. Data for SR, SRB, AF, and AFB are shown in top, second, third, and bottom panels respectively. Columns I, II, and III show illustrative frames from the 2D simulations. Column VI shows trace of spiral wave tip. Column V shows AP traces from representative locations in the 2D sheet, and Column VI shows the frequency spectrum in the AP traces.

Atrial selective drugs which target atrial specific ion channels, such as  $I_{Kur}$ , provide an attractive target for drug therapy in the treatment of AF without adversely affecting the electrophysiological function of the ventricles. However, while blocking of the  $I_{Kur}$  has been shown experimentally, and in our simulations to prolong APD in cardiac myocytes which have undergone AF induced electrical remodelling, current pharmacological agents which block  $I_{Kur}$  (e.g. Vernakalant, AZD7009, and AVE0118) also block the sodium current ( $I_{Na}$ ) and the transient outward current ( $I_{to}$ ), resulting in long term complications if administered for extended durations. Our simulations confirmed that the blockage for patients who have undergone electrical remodelling may limit the occurrence of AF and aid in rhythm control but is not effective once a spiral wave has been initiated.

The potential limitations of the CRN model used in this study have been discussed previously [8, 16]. A limitation of our 3D simulations is the absence of electrical heterogeneity in the atria, and only consists of atrial cell types while it is known that cells in different regions have different electrophysiological properties [13]. The spatial heterogeneities due to fiber orientation are also neglected in our simulations and we have implemented a uniform diffusion tensor in our

simulations.

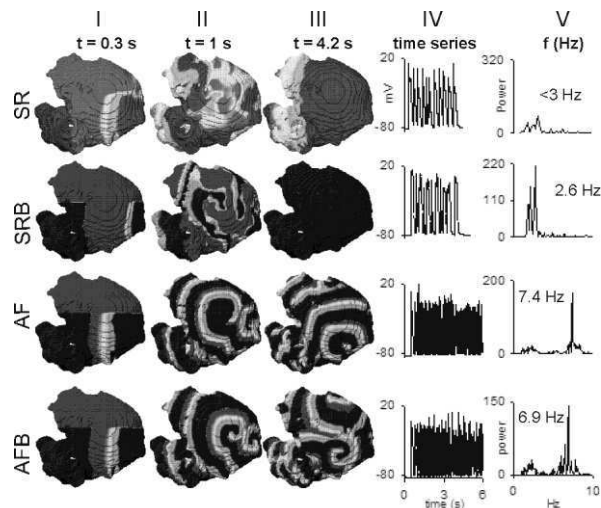


Figure 4 Scroll waves in 2D homogenous human atria. Data for SR, SRB, AF, and AFB are shown in top, second, third, and bottom panels respectively. Column I, II, and III illustrate the simulation. Column IV shows AP traces from representative locations in the 3D model, and Column VI shows the frequency spectrum in the AP traces.

## Acknowledgements

This work was supported by EPSRC and Wellcome Trust (UK) grants (WT/081809/Z/06/Z).

## References

- [1] Nattel S, Singh BN. Evolution, mechanisms, and classification of antiarrhythmic drugs: focus on class III actions. *Am J Cardiol.* 1999; 84(9A):11R-9R.
- [2] Tamargo J, Valenzuela C, Delpon E. New insights into the pharmacology of sodium channel blockers. *Eur Heart J.* 1992; 13 Suppl F:2-13.
- [3] Tamargo J, Caballero R, Delpon E. Pharmacological approaches in the treatment of atrial fibrillation. *Curr Med Chem.* 2004; 11(1):13-28.
- [4] Tamargo J, Caballero R, Gomez R, Delpon E. I(K<sub>ur</sub>)/Kv1.5 channel blockers for the treatment of atrial fibrillation. *Expert Opin Investig Drugs.* 2009; 18(4):399-416.
- [5] Brendel J, Peukert S. Blockers of the Kv1.5 channel for the treatment of atrial arrhythmias. *Curr Med Chem Cardiovasc Hematol Agents.* 2003; 1(3):273-87.
- [6] Ford JW, Milnes JT. New drugs targeting the cardiac ultra-rapid delayed-rectifier current (I<sub>Kur</sub>): rationale, pharmacology and evidence for potential therapeutic value. *J Cardiovasc Pharmacol.* 2008; 52(2):105-20.
- [7] Wettwer E, Hala O, Christ T, Heubach JF, Dobrev D, Knaut M, et al. Role of I<sub>Kur</sub> in controlling action potential shape and contractility in the human atrium: influence of chronic atrial fibrillation. *Circulation.* 2004; 110(16):2299-306.
- [8] Courtemanche M, Ramirez RJ, Nattel S. Ionic mechanisms underlying human atrial action potential properties: insights from a mathematical model. *Am J Physiol.* 1998; 275(1 Pt 2):H301-21.
- [9] Kharche S, Seemann G, Margetts L, Leng J, Holden AV, Zhang H. Simulation of clinical electrophysiology in 3D human atria: a high-performance computing and high-performance visualization application. *Concurrency and Computation: Practice and Experience.* [Journal Article]. 2008; 20(11):10.
- [10] Zhang H, Garratt CJ, Zhu J, Holden AV. Role of up-regulation of I<sub>K1</sub> in action potential shortening associated with atrial fibrillation in humans. *Cardiovasc Res.* 2005; 66(3):493-502.
- [11] Kharche S, Garratt CJ, Boyett MR, Inada S, Holden AV, Hancox JC, et al. Atrial proarrhythmia due to increased inward rectifier current (I<sub>K1</sub>) arising from KCNJ2 mutation--a simulation study. *Prog Biophys Mol Biol.* 2008; 98(2-3):186-97.
- [12] Kharche S, Zhang H. Simulating the effects of atrial fibrillation induced electrical remodeling: a comprehensive simulation study. *Conf Proc IEEE Eng Med Biol Soc.* 2008; 2008:593-6.
- [13] Seemann G, Hoper C, Sachse FB, Dossel O, Holden AV, Zhang H. Heterogeneous three-dimensional anatomical and electrophysiological model of human atria. *Philos Transact A Math Phys Eng Sci.* 2006; 364(1843):1465-81.
- [14] Kharche S, Seemann G, Leng J, Holden AV, Garratt CJ, Zhang H. Scroll Waves in 3D Virtual Human Atria: A Computational Study. In: Seemann FBSaG, editor. LNCS; 2007. p. 129-38.
- [15] Workman AJ, Kane KA, Rankin AC. The contribution of ionic currents to changes in refractoriness of human atrial myocytes associated with chronic atrial fibrillation. *Cardiovasc Res.* 2001; 52(2):226-35.
- [16] Cherry EM, Evans SJ. Properties of two human atrial cell models in tissue: restitution, memory, propagation, and reentry. *J Theor Biol.* 2008; 254(3):674-90.

Address for correspondence:

Name: Dr. Sanjay Kharche

Full postal address: School of Physics and Astronomy, University of Manchester, Manchester, UK, M13 9PL

E-mail address: Sanjay.Kharche@manchester.ac.uk